Desalination and Water Treatment
www.deswater.com
doi: 10.5004/dwt.2022.28621

266 (2022) 91–100
August

Removal of Cr(III) from tanning effluent using adsorbent prepared from peanut shell

Fatema-Tuj-Zohra[a,b], Sobur Ahmed[a,b], Razia Sultana[a], Md. Nurnabi[b,*], Md. Zahangir Alam[b,*]

[a]*Institute of Leather Engineering and Technology (ILET), University of Dhaka, Bangladesh, emails: fatema.ilet@du.ac.bd (Fatema-Tuj-Zohra), soburahmed@du.ac.bd (S. Ahmed), raziasultana.du31@gmail.com (R. Sultana)*
[b]*Department of Applied Chemistry and Chemical Engineering, University of Dhaka, Bangladesh, Tel. +8801711577225; Fax: +880-2-9667222; email: nabi@du.ac.bd (Md. Nurnabi), zahangir@du.ac.bd (Md. Z. Alam)*

Received 29 January 2022; Accepted 30 May 2022

ABSTRACT

This article describes the development of an adsorbent from peanut shell (PNS) for removing Cr(III) from tannery effluents. Adsorbent was prepared by pyrolysis of peanut shell followed by activation with NaOH and was characterized by different analytical methods. Adsorption capacity and removal rate of Cr(III) were determined. The adsorption capacity of activated PNS was investigated through batch experiments with the effect of pH, adsorbent doses, contact time, initial concentration, and temperature. Adsorption capacity and rate of removal of Cr(III) were 74.79 mg/g and 54.21%, respectively. The highest adsorption capacity (q_m) calculated from Langmuir isotherm was 104.82 mg/g. Adsorption isotherm of Cr(III) on PNS was studied by Langmuir and Freundlich models which revealed that Langmuir model fitted the best with a R^2 value of 0.999. The adsorption kinetics of Cr(III) on PNS followed pseudo-second-order reaction model with a R^2 value of 0.9979. The experimental data of Cr(III) adsorption were also fitted well with the pseudo-second-order kinetic model. Various physico-chemical parameters of chrome tanning effluent were also evaluated prior to and subsequent to adsorption.

Keywords: Activated carbon; Adsorption capacity; Adsorption isotherm; Peanut shell; Tannery effluent

1. Introduction

One of the most important environmental concerns of this century is the contamination of surface water with heavy metals. As we know, heavy metals cannot be degraded or destroyed; hence they are interminable in all parts of the environment [1,2]. Worldwide water sources are going under serious threat due to unplanned industrialization and urbanization. In the developing countries like Bangladesh, there is a tendency to set up industries beside the water bodies, and discharges untreated industrial waste to the surface water. Chromium compounds have gained extensive applications in leather tanning, textile dyeing, wood preservation, printing inks, paints and pigments, and metal plating [3]. Tannery effluents contain high chromium content and other organic and inorganic pollutants of a very heterogeneous group of elements in their properties and functions [4].

In leather tanning, 60%–70% of employed chromium is consumed by leather and the rest 30%–40% remains in the spent tan liquor [5]. It is reported that the waste and spent liquor from tanneries contain 10–50 and 2,900–4,500 mg/L of chromium, respectively [6]. The discharged unexploited

* Corresponding authors.

Cr from chrome tanning causes serious risk to the environment. In particular, the hexavalent chromium poses an urgent warning since it is highly reactive and carcinogenic [7]. Hexavalent chromium is 1,000 times higher toxic than trivalent chromium because of its solubility and mobility [8]. Trivalent chromium is not so harmful, though large amounts of chromium ion (Cr^{3+}) can affect the ecological environment remarkably [9]. The maximum permissible level of Cr(VI) is 0.05 mg/L, and the total chromium is below 2 mg/L in accordance with the United States Environmental Protection Agency (UNFPA) [10]. Adsorption is considered the most convenient processes for toxic metals removal from industrial wastewater as adsorbents are easily available in the form of industrial, biological and domestic waste, usable after regeneration, useful in wide range of pH, eco-friendly and low-cost [11–17]. Activated carbons are the mostly used adsorbents to remove toxic substances from water [18]. There are some other adsorbents, such as hydrophobic cross-linked polyzwitterionic acid (HCPZA) resin, polyamide grafted eggshell (CMP), silica-multiwall carbon nanotubes (SiO_2-CNT), polyamide modified baghouse dust nanocomposite (PMBHD) [19–21]. It is well known that trivalent chromium salt, basic chromium sulphate is used in tanning of hides and skins. Unless oxidized it is exist in the effluent and environment as Cr(III) form which is required to be removed and reused. The sustainability of leather sector in Bangladesh is facing a big challenge for the removal of chromium from tannery effluent. However, most of the previous research focused on treatment of Cr(VI) and a very limited research is carried out for used Cr(III) removal from tannery effluent with adsorbents prepared from agro-waste. Some research groups reported the adsorption capacity of saw dust (5.52 mg/g), paper mill lignin (17.97 mg/g) and endocarp of açaí berry (1.211 mg/g) [22], although the adsorption capacities were not satisfactory. In this research, the preparation of a cost-effective and efficient adsorbent from peanut agro-waste and its adsorption performance, kinetics and thermodynamics were studied in detail.

2. Experimental

2.1. Materials

Peanut shells were collected from the local market at Hazaribagh, Dhaka, Bangladesh. They were stripped off and cleaned with deionized water to eliminate dust and other contaminants, and dehydrated completely. Chromium(III) sulfate [$Cr_2(SO_4)_3{\cdot}6H_2O$] as the source of Cr(III) was collected from Qualikems Fine Chem., India. Sulfuric acid (98%) and NaOH were procured from Merck, Germany. All chemicals were used as received without further treatment.

2.2. Instruments

Fourier transform infrared spectroscopy (FTIR (8400S Shimadzu, Japan), scanning electron microscopy (SEM (JSM-6490LA, JEOL, USA) were used for the characterization of the adsorbents. Concentration of Cr(III) were determined with ICPMS (7900 Agilent Technologies International Ltd, Japan) and UV-VIS Spectrophotometer (UV-1700 Pharma Spec, SHIMADZU).

2.3. Preparation of activated peanut shells

Dried peanut shells (250 g) were pyrolyzed in a vertical tube furnace at 500°C ± 10°C for 2 h and then chemically activated with analytical grade NaOH. A 25% NaOH solution was added to charcoal (138 g) with stirring and left for 24 h to complete chemical activation. Then it was washed with distilled water and dried in an oven at 110°C–115°C. Carbonization enriched carbon content and created a primary porosity, and activation enlarged the pores [23]. The activated dried peanut shells (PNS) were then powdered and used in this study.

2.4. Batch adsorption studies

Chromium(III) stock solution was prepared by dissolving [$Cr_2(SO_4)_3{\cdot}6H_2O$] salt with deionized water and the necessary working solutions were prepared by dilution. Initial concentration of [$Cr_2(SO_4)_3{\cdot}6H_2O$] solutions (32.06, 69.19, 135.43, 187.57, 271.74, 301.26, and 363.47 mg/L) were determined by ICPMS and developed the calibration curve with UV-Visible Spectroscopy at 421 nm wavelength. A series of conical flasks in a orbital shaker with 25 mL of [$Cr_2(SO_4)_3{\cdot}6H_2O$] solution and fixed adsorbent doses (2.5 g/L) were used for conducting batch experiment. In order to determine the effects of pH, adsorbent dose, contact time, initial Cr(III) concentration, and temperature on adsorption of Cr(III), multiple experiments were conducted. The pH of solution was controlled at 3.0–5.0 with the addition of H_2SO_4 and NaOH [24]. The initial concentration of the solution for the study was 256 ppm. All batch experiments were performed at a fixed speed of orbital shaker (160 rpm). Whatman filter paper was used to filtrate and then the filtrate was analyzed with UV-Visible spectroscopy. After completion of batch experiments, a chrome tanning effluent sample was studied with the prepared adsorbent for Cr(III) removal and adsorption capacity was calculated by the following equation.

$$q_t = \frac{(C_0 - C_t)V}{W} \tag{1}$$

where C_0 = initial concentration of Cr^{3+} solution (ppm), C_t = concentration of Cr^{3+} solution (ppm) at time t, V = volume (L) of the Cr^{3+} solution and W = mass (g) of the adsorbent.

Eq. (2) was used to calculate equilibrium adsorption capacity, q_e (mg/g).

$$q_e = \frac{(C_0 - C_e)V}{W} \tag{2}$$

where C_e = concentration of Cr^{3+} solution (ppm) at equilibrium.

Percentage (%) of Cr(III) removal was determined following Eq. (3).

$$\%\text{Removal} = \frac{(C_0 - C_e)}{C_0} \times 100 \tag{3}$$

where C_0 and C_e is the initial and equilibrium concentration of Cr(III) solution, respectively.

3. Results and discussion

3.1. Characterization

In this work, pyrolyzed nut shell (PNS-1) and activated pyrolyzed nut shell (PNS-2) were prepared and were characterized with SEM, X-ray diffraction (XRD) and FTIR spectroscopy. Pyrolyzed activated nut shell after adsorption (PNS-3) of Cr(III) was also characterized similarly.

3.1.1. FTIR analysis

It is known that peanut shell is composed of cellulose, hemicelluloses and lignin. PNS undergoes different changes during activation and the Cr(III) adsorption process. The vibrational changes of PNS after activation and adsorption process were examined by means of FTIR spectroscopy. The FTIR spectra of PNS-1, PNS-2 and PNS-3 are depicted in Fig. 1.

A several functional groups were relocated at different frequency level and disappeared after chemical activation and adsorption [25]. Broad peaks centered at 3,332; 3,325 and 3,340 cm^{-1} were detected in the IR spectra of PNS-1, PNS-2 and PNS-3, respectively owing to the presence of –OH groups [26]. Peaks at 1,712; 1,728 and 1705 cm^{-1} indicating –C=O groups were also present in the IR spectra [17,27]. C–H stretching vibrations were found at 2,970 and 2,885 cm^{-1} in PNS-1; 2,939 and 2,870 cm^{-1} in PNS-2 and 2,970 and 2,885 cm^{-1} in PNS-3. The peak at 1,373; 1,350 and 1373 cm^{-1} in IR spectra of PNS-1, PNS-2 and PNS-3, respectively were because of crystalline cellulose.

3.1.2. SEM analysis

Surface morphology of activated PNS was investigated using SEM. In Fig. 2 the SEM image shows the lamellar, irregular and heterogeneous structure and numerous cavities of activated PNS. These features of adsorbent support the metal adsorption process in aqueous media.

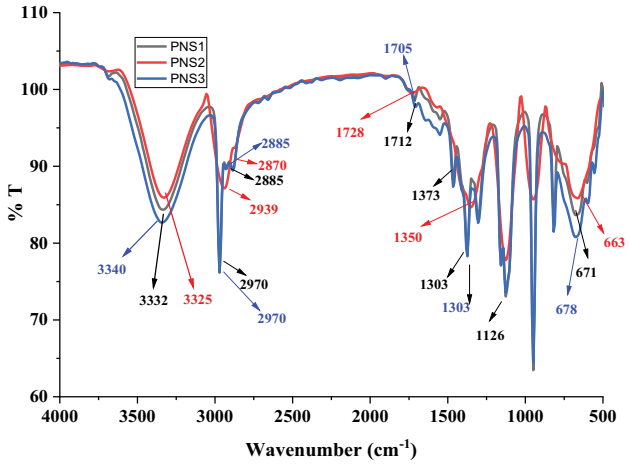

Fig. 1. FTIR spectra of pyrolyzed nut shell (PNS-1), NaOH activated pyrolyzed nut shell (PNS-2), Cr(III) loaded NaOH activated pyrolyzed nut shell (PNS-3).

3.1.3. XRD analysis

The XRD pattern of activated PNS is shown in Fig. 3. No well-defined peak related to crystalline phase was observed in the X-ray diffraction pattern. It shows a typical peak of carbonaceous compound. A hump in the range of 2θ = 20°–30° and a peak at 2θ = 22.8° were observed due to the amorphous structure with a high degree of disorder of PNS. The broad and weak peaks observed in XRD pattern of PNS represent the presence of amorphous carbon [28].

3.2. Effect of adsorption capacity of PNS on Cr(III)

3.2.1. Effect of pH

Fig. 4 interprets the effect of pH on adsorption capacity of PNS and it exhibits that Cr(III) adsorption capacity of PNS was increased with increasing the pH of solution from 3.5 to 5.0. The positively charged metal ion adsorption is decreased at low pH due to protonation of carboxyl groups. On the other hand, adsorption is augmented at higher pH (above 4.00) due to negatively charged carboxylate (–COO–) ligands as a result of deprotonation of carboxyl groups resulting in an attraction of metal ions [29]. The surface negativity of PNS was increased with increasing pH, which was observed from zeta potential value (Fig. 4c).

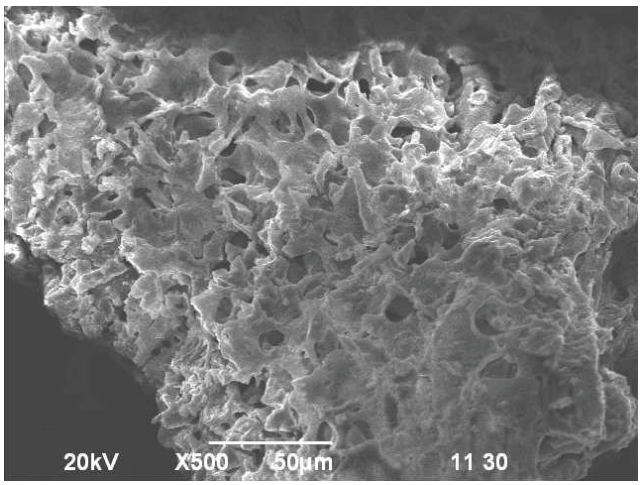

Fig. 2. SEM image of NaOH activated PNS.

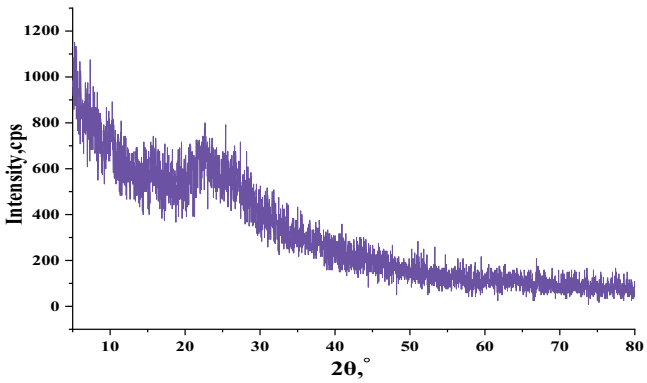

Fig. 3. XRD patterns of PNS.

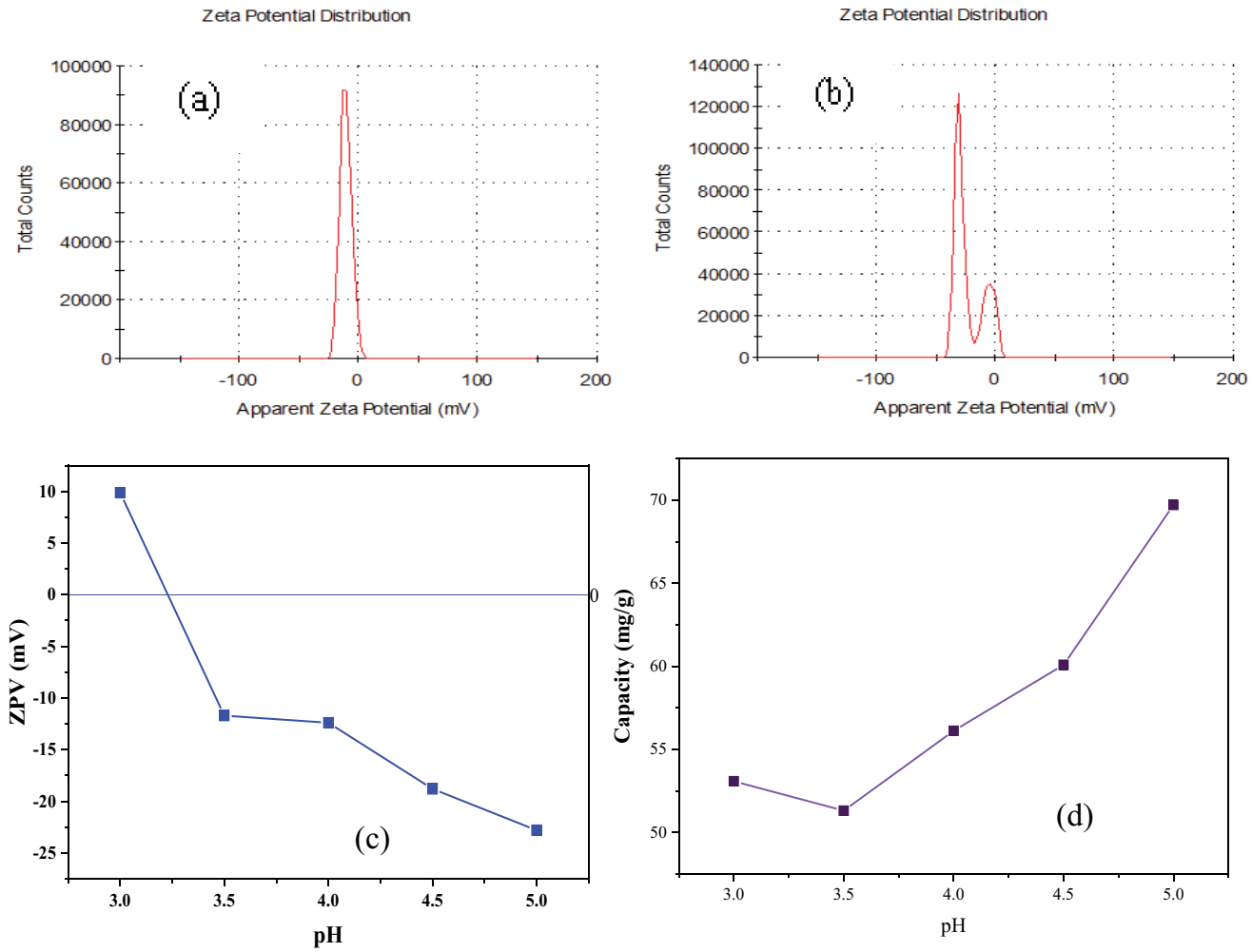

Fig. 4. Zeta potential value of PNS (a) at pH 3.5 (–10.2 mV), (b) at pH 5.0 (–22.8 mV), (c) pH effect on ZPV, and (d) pH effect on Cr(III) adsorption.

Cr(III) species as $Cr(H_2O)_6^{3+}$, $Cr(OH)(H_2O)_5^{2+}$ and $Cr(OH)_2(H_2O)_4^{+}$ generally bear positive charges and is absorbed by the negatively charged adsorbents [30]. In this work, all the batch experiments were carried out at pH 5.0 to attain possible highest adsorption capacity without any precipitation of Cr(III) [31]. Moreover, Cr(III) can be precipitated and separated as $Cr(OH)_3$ from aqueous solution at pH > 6.0 [32].

3.2.2. *Effect of adsorbent dose*

Adsorption capacity and % of removal as a function of adsorbent (PNS) dose is presented in Fig. 5. Different dosages of PNS were employed to optimize the doses for maximum amount of Cr(III) removal from aqueous solution.

Adsorption capacity of PNS decreased from 75.16 to 52.65 mg/g with increasing the doses from 1.5 to 4.0 g/L, whereas percentage of removal was increased from 46.86% to 87.53%. An increase in percentage Cr(III) removal is assumed because of the increment of available adsorption sites, while the availability of remaining unsaturated sites decreased adsorption capacity [33].

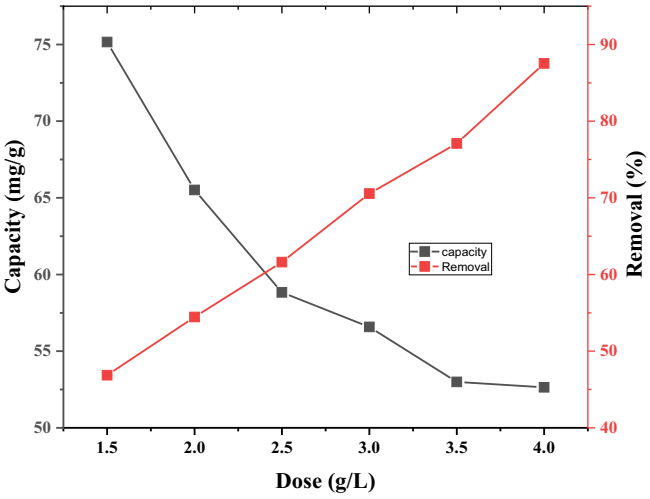

Fig. 5. Effect of doses on adsorption capacity and removal of Cr(III).

3.2.3. Effect of contact time and concentration on adsorption

Various concentrations of Cr(III) solutions, that is, 125, 196, 278, 330, and 370 mg/L were used to find the initial concentration effect on adsorption capacity. 2.5 g/L NaOH treated PNS was added to 25 mL Cr(III) sulfate [$Cr_2(SO_4)_3 \cdot 6H_2O$] solution and was shake in an orbital shaker at room temperature. Percentage (%) removal and adsorption capacity were determined at different time interval to find out the equilibrium point. The percentage of Cr(III) removal was decreased as the sorption sites get saturated by a higher amount of metal ions. A high percentage of Cr(III) removal was detected at low Cr(III) ions concentration as a result of availability of adsorption sites.

Fig. 6 shows that the adsorption capacity increased with increasing the duration of adsorption. The percentage of Cr(III) removal was high initially, probably because of the accessibility of bigger contact area of activated PNS. It is found that adsorption reached at equilibrium almost after 240 min. It is also observed that adsorption capacity was increased and % of removal was decreased with the increasing of metal ion concentration. In the case of 125 ppm initial Cr(III) concentration, adsorption capacity and % of removal was 37.22 mg/g and 74.49% while at 196, 278, 330 and 370 ppm initial concentration, adsorption capacity and % of removal were 53.51 mg/g and 68.46%, 68.53 mg/g and 61.94%, 74.11 mg/g and 56.49%, 79.00 mg/g and 53.79%, respectively. The highest adsorption capacity (79.00 mg/g) was obtained in case of 370 ppm solution.

3.3. Adsorption isotherm of PNS

Adsorption isotherm shows a relationship between the quantities of adsorbate (mg) removed from the liquid-phase with unit mass of an adsorbent (g) at a certain temperature [34,35]. Langmuir and Freundlich isotherm models were applied to study the adsorption capacity of activated PNS for Cr(III) removal from aqueous solution.

3.3.1. Langmuir isotherm

It represents the monolayer adsorption process on a homogeneous surface without interaction between adsorbed adjacent molecules. The following Langmuir equation was employed to study the adsorption isotherm of Cr(III) on PNS.

$$\frac{C_e}{q_e} = \frac{1}{q_m b} + \frac{1}{q_m} C_e \tag{4}$$

where q_e is the monolayer saturation adsorption capacity of the adsorbent (mg/g), C_e is the equilibrium concentration (mg/L), b is the Langmuir adsorption constant (L/mg) and q_m is the equilibrium adsorption capacity. Therefore, a plot of C_e/q_e vs. C_e should be a straight line with a slope ($1/q_m$) and an intercept as $1/q_m b$. The constant values of q_m and b were calculated and reported in Table 1. A dimensionless equilibrium parameter, the separation factor R_L, was also calculated for further analysis of Langmuir isotherm using Eq. (5) [36].

$$R_L = \frac{1}{1 + C_m b} \tag{5}$$

where b = Langmuir adsorption constant (L/mg) and C_m = maximum concentration (mg/L) of the Cr(III) ion. The R_L value at 0–1 indicates favorable and $R_L > 1$ indicates unfavorable adsorption whereas, $R_L = 1$ indicates linear adsorption. The adsorption process is irreversible if the R_L value is 0 [37].

Fig. 7a shows a linear relation between C_e/q_e and C_e and a high correlation coefficient (R^2 = 0.999) which indicates a good agreement between the parameters. The value

Table 1
Isotherm constants for Cr(III) adsorption on PNS

Langmuir constants	Values	Freundlich constants	Values
q_m (mg/g)	104.820	K_F	8.221
b (L/mg)	0.017	N	2.255
R^2	0.999	R^2	0.986
R_L	0.138		

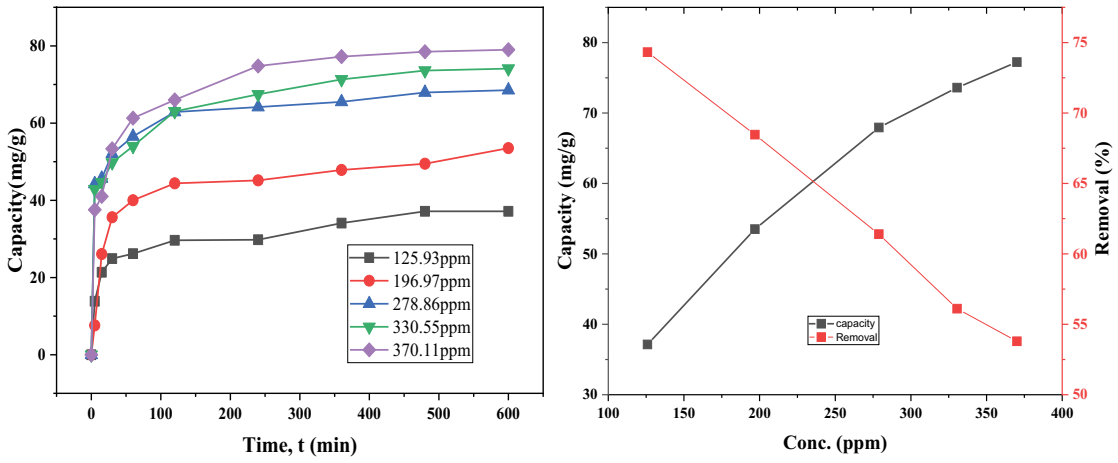

Fig. 6. Effect of contact time and initial concentration on adsorption.

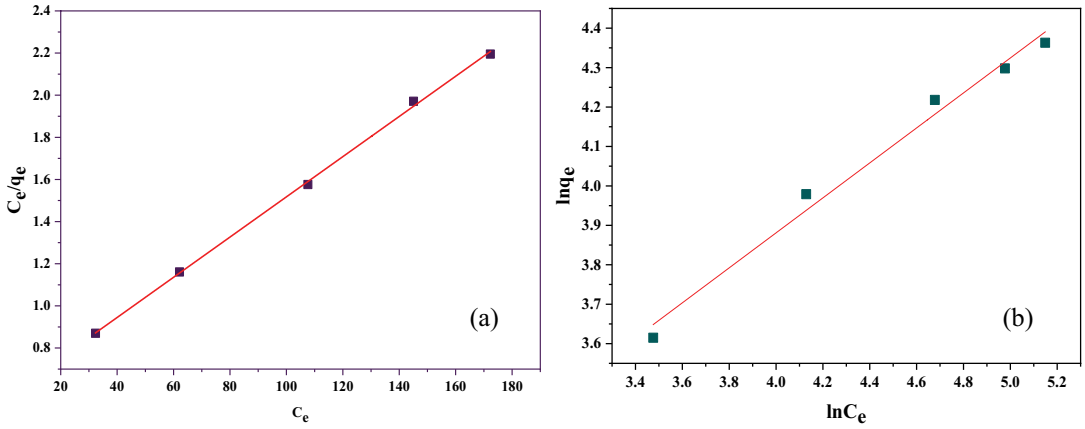

Fig. 7. (a) Langmuir and (b) Freundlich adsorption isotherm plots for adsorption of Cr(III) on NaOH treated PNS.

of parameter R_L of this study is 0.138 ($0 < R_L < 1$) which is consistent with the condition of a favorable adsorption.

3.3.2. Freundlich model

Freundlich isotherm corresponds to the adsorption of heavy metal ions by multilayer adsorption process on a heterogeneous surface. This model is expressed by Eq. (6) as follows:

$$\ln q_e = \ln K_F + \frac{1}{n}\ln C_e \tag{6}$$

where q_e is the equilibrium adsorption capacity, K_F the sorption capacity (mg/g), C_e is the equilibrium concentration (mg/L), and n is an empirical parameter. Freundlich constant "n" reveals the surface heterogeneity and the favorability of adsorption. The adsorption is favorable if the "n" value is less than 10 and higher than 1 [38]. The plot of $\ln q_e$ vs. $\ln C_e$ shown in Fig. 7b was obtained by plotting the experimental data. Values of K_F, n, and correlation coefficients (R^2) are established and presented in Table 1.

The graphical representation of $\ln q_e$ and $\ln C_e$ showed that the plot is a straight line with an intercept of $\ln K_F$ and a slope $1/n$. The value of correlation coefficient R^2 is 0.986 which revealed the surface heterogeneity of PNS and multilayer adsorption process.

3.4. Kinetic studies of the adsorption of Cr(III) on PNS

The adsorption kinetics of Cr(III) on PNS was studied to determine the promptness of ion transfer from aqueous to solid phase and to determine the required time for reaching equilibrium between the phases [39]. In this research, both the pseudo-first-order and pseudo-second-order kinetics models were exploited to study the adsorption of Cr(III) ion on NaOH treated PNS.

3.4.1. Pseudo-first-order model

The adsorption of an adsorbent from an aqueous solution is studied by widely used pseudo-first order equation developed by Lagergren. In this model it is assumed that rate of change of solute uptake is directly proportional to the difference in saturation concentration and the amount of solid uptake with time.

$$\frac{dp}{dt} = k\left(q_e - q_t\right) \tag{7}$$

when $q_t = 0$ at $t = 0$, Eq. (7) is integrated and then rearranged to achieve the following linear form.

$$\log\left(q_e - q_t\right) = \log q_e - \frac{k_1}{2.303}t \tag{8}$$

where q_e and q_t are the amount of solute adsorbed at equilibrium per unit weight of adsorbent (mg/g) and at any time (mg/g), respectively and k_1 is the adsorption constant. Experimental data were plotted according to Eq. (8) and is demonstrated in Fig. 8a.

3.4.2. Pseudo-second-order model

The following equation is represented the pseudo-second-order kinetics model [40]:

$$\frac{t}{q_t} = \left(\frac{1}{k_2 q_e^2}\right) + \left(\frac{1}{q_e}\right)t \tag{9}$$

The plot of t/q_t vs. t showed a linear relationship with an excellent correlation coefficient (R^2) value of 0.9979 (Fig. 8b). Therefore, the experimental data also fitted well with the pseudo-second-order kinetic model. The value of q_e and k_2 were determined from the slope and intercept of the plot. The values of different parameters of both the kinetic models are shown in Table 2.

The data presented in Table 2 revealed that pseudo-second-order kinetic model described the experimental data of adsorption of Cr(III) on PNS better than pseudo-first-order kinetic model. It was also found that correlation coefficient (R^2) value of pseudo-second-order kinetic model was also better than that of pseudo-first-order kinetic model. In case of pseudo-second-order kinetic model the

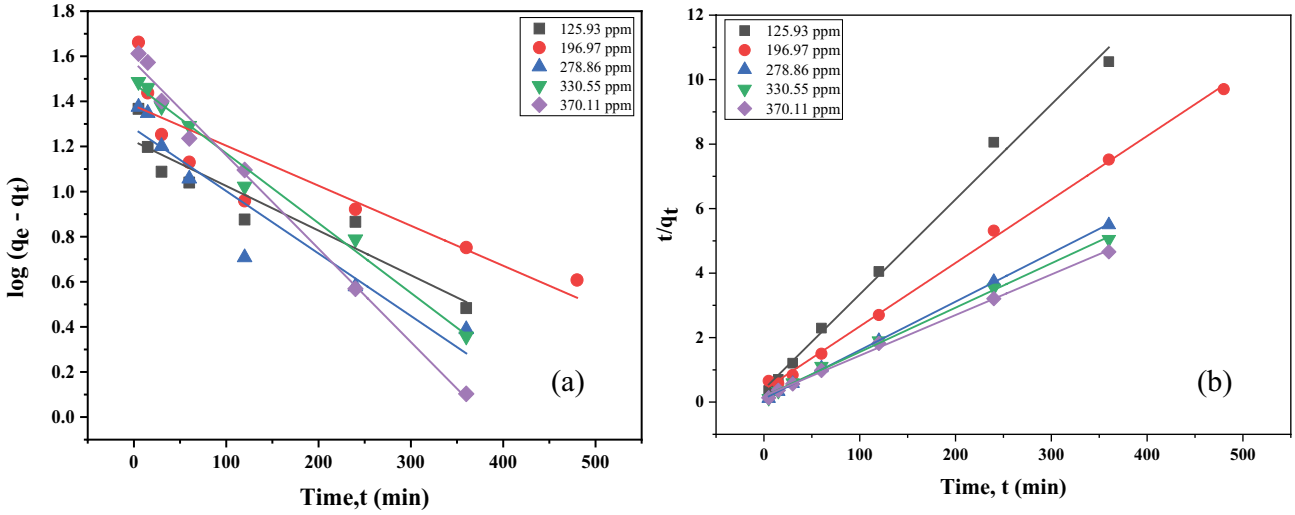

Fig. 8. (a) Pseudo-first-order and (b) pseudo-second-order kinetic plots for Cr(III) ions adsorption on PNS at 25°C.

Table 2
Pseudo-first-order and pseudo-second-order rate constants for Cr(III) ion adsorption

Kinetic model	Parameters	125 ppm	196 ppm	278 ppm	330 ppm	370 ppm
Pseudo-first-order	q_e* (mg/g)	37.14	49.46	67.94	73.60	78.50
	k_1	0.00456	0.00410	0.00637	0.00712	0.00953
	R^2	0.875	0.805	0.894	0.989	0.990
Pseudo-second-order	q_e** (mg/g)	16.71	24.05	19.02	30.14	37.60
	k_2	0.00128	0.00078	0.00162	0.00087	0.00078
	R^2	0.989	0.995	0.999	0.998	0.998
	q_e** (mg/g)	36.82	53.28	68.12	74.68	80.52

*Experimental;
**Theoretical.

theoretical q_e values agreed well with the experimental values of q_e. Thus, Cr(III) adsorption on PNS is followed by pseudo-second-order kinetic model.

3.5. Thermodynamics of adsorption of Cr(III) on PNS adsorbent

Thermodynamics of Cr(III) adsorption on PNS was also studied and adsorption experiments were accomplished at temperatures of 293, 308, 323 and 338 K to detect thermodynamic parameters, for example, Gibbs free energy ($\Delta G°$), enthalpy ($\Delta H°$), and entropy ($\Delta S°$) by the following equations:

$$\Delta G° = -RT \ln K_d \tag{10}$$

$$\ln K_d = \frac{-\Delta H°}{RT} + \frac{\Delta S°}{R} \tag{11}$$

$$\Delta S° = -\frac{\Delta G° - \Delta H°}{T} \tag{12}$$

where K_d = the distribution coefficient of adsorbent obtained by q_e/C_e. R = the gas constant (8.314 kJ/mol); T = adsorption temperature (K). $\Delta H°$ and $\Delta S°$ is determined from the plot between $\ln K_d$ and $1/T$ [41] which is demonstrated in Fig. 9b.

All thermodynamic parameters calculated for the adsorption Cr(III) on PNS is shown in Table 3.

The values of $\Delta G°$ for Cr(III) adsorption on PNS at the temperatures of 293, 308, 323 and 338 K were found to be –2.015, –1.345, –0.559 and –0.171 kJ/mol, respectively. The negative values of $\Delta G°$ revealed that Cr(III) adsorption on PNS was favorable and spontaneous. The negative value of $\Delta H°$ indicated that the Cr(III) adsorption on PNS was exothermic in nature. The negative value of $\Delta S°$ revealed the decrease in randomness at the solid/solute interface during the Cr(III) adsorption on PNS [42].

3.6. Regeneration of used PNS adsorbent

The possibility of re-using PNS as adsorbent was investigated. Cr(III) loaded PNS was regenerated using 1.0 M H_2SO_4 and NaOH solution thrice. Experimental pH, adsorbent dose and other conditions were at optimum level.

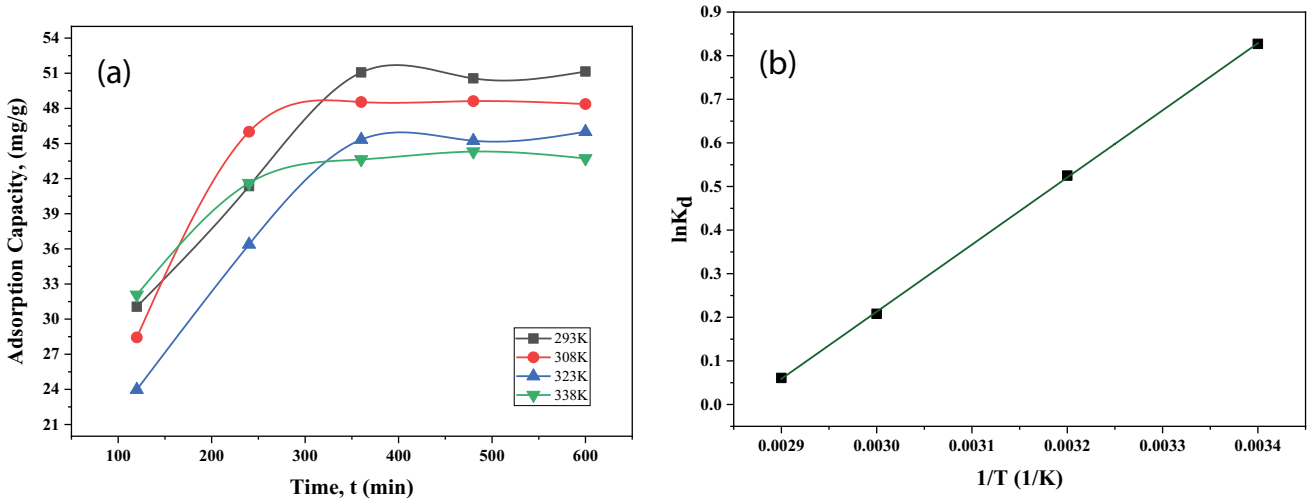

Fig. 9. (a) Adsorption capacity at different temperature and (b) plots of lnK_d vs. 1/T for Cr(III) adsorption by PNS.

Table 3
Thermodynamic parameters for adsorption of Cr(III) on PNS

T (K)	$\Delta G°$ (kJ/mol)	$\Delta H°$ (kJ/mol)	$\Delta S°$ (kJ/mol)
293	–2.015	–12.799	–0.036
308	–1.345		
323	–0.559		
338	–0.171		

Table 4
Adsorption capacity of regenerated PNS

Regeneration of the adsorbent	Capacity (mg/g)
NaOH activated PNS	61.86
1st recycle	48.62
2nd recycle	28.95
3rd recycle	22.71

The results of regeneration studies are tabulated in Table 4 which shows that adsorption capacity gradually decreased from 48.62 to 22.70 mg/g. It is evident that regenerated PNS can reuse for Cr(III) removal from aqueous solution.

3.7. Real sample analysis

The effluent of chrome tanning was collected from Reliance Tannery, Tannery Industrial Estate Dhaka (TIED), Hemayetpur, Savar, Dhaka. In order to study the adsorption of Cr(III) ions from the concentrated chrome tanning effluent, 12.5 g of activated PNS was inserted to 500 mL of effluent followed by shaking in an orbital shaker at atmospheric temperature for 4 h at pH 5.0. The results of the physico-chemical parameters before and after adsorption are shown in Table 5. It is observed that 54.19% Cr(III) was removed from real sample. After adsorption with PNS the water quality parameters of collected tannery effluent such as total dissolved solids (TDS), electrical conductivity (EC), biochemical oxygen demand (BOD_5), chemical oxygen demand (COD), etc. were also reduced significantly.

Table 5
Physico-chemical parameters of tannery effluents before and after adsorption

Parameters	Before adsorption	After adsorption	% of removal
Cr(III) (ppm)	3,477.50	1,592.72	54.19
Adsorption capacity (mg/g)	–	74.79	–
pH	4.1	5.2	–
TDS (ppm)	5,135	2,203	57.09
EC (μS/cm)	10,165	5,421	46.67
NaCl (%)	17.60	8.30	52.84
BOD_5 (ppm)	4,643	2,238	51.79
COD (ppm)	12,164	5,669	53.40

3.8. Plausible mechanism of adsorption of Cr(III) on PNS

The study on adsorption mechanism is critical for the removal of metal from aqueous solution. The electrostatic interaction between oppositely ionized particles through different bond formations, such as hydrogen bonding, Van der Waals force, dipole-dipole induction, ion-exchange, etc. can be dealt with sorption mechanism. The surface chemistry and pore density/volume are:

The two topmost variables, that is, the surface chemistry and the pore density/volume plays significant influences throughout the sorption process of a solute onto an adsorbent surface. It was revealed from previous study that the functional groups like, carboxyl, hydroxyl, methoxy, and phenolic groups present in pyrolyzed peanut shell, which could attach and remove metallic ions and the other pollutants from wastewater [43,44]. In general Cr ions form hexacoordinate complexes. In the present study, it is

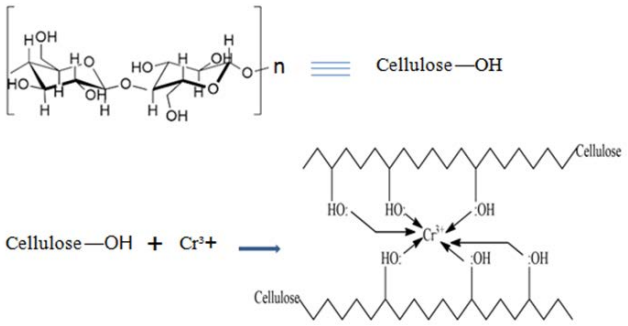

Fig. 10. Plausible mechanism of Cr(III) adsorption on to activated PNS.

assumed that carboxylate groups containing PNS cellulose form hexacoordinate complexes by capturing Cr(III) ions from the solution (Fig. 10).

4. Conclusion

In this work, an adsorbent was developed by pyrolysis of peanut shell followed by activation with NaOH and was characterized with FTIR, SEM and XRD. This study showed that PNS treated with NaOH could be a suitable adsorbent for Cr(III) removal from aqueous solution. Adsorption of Cr(III) on PNS was explained well by the Langmuir model. The maximum adsorption capacity of PNS for Cr(III) was 104.82 mg/g. The adsorption of Cr(III) was influenced by pH of solution and the optimum pH was found 5.0. Pseudo-second-order kinetic model described the experimental data better than the pseudo-first-order kinetic model. $\Delta H°$ and $\Delta S°$ value were found –12.799 and –0.0366 kJ/mol that confirmed the feasibility of adsorption. The capacity of PNS for Cr(III) adsorption from tannery effluent was found 74.79 mg/g and the percentage of removal was 54.21%. The regeneration of the adsorbent was very simple and regenerated PNS showed good adsorption capacity (48.62%). Thus, pyrolyzed and NaOH treated peanut shell could be a potential adsorbent for the removal of Cr(III) from tannery effluents.

Acknowledgements

The authors would like to acknowledge the financial supports from the Ministry of Science and Technology and the Ministry of Education, the Government of the People's Republic of Bangladesh.

References

[1] S. Tamjidi, H. Esmaeili, B.K. Moghadas, Application of magnetic adsorbents for removal of heavy metals from wastewater: a review study, Mater. Res. Express., 6 (2019) 102004, doi: 10.1088/2053-1591/ab3ffb.
[2] X. Liu, R. Ma, X. Wang, Y. Ma, Y. Yang, L. Zhuang, S. Zhang, R. Jehan, J. Chen, X. Wang, Graphene oxide-based materials for efficient removal of heavy metal ions from aqueous solution: a review, Environ. Pollut., 252A (2019) 62–73.
[3] H. Zhang, H. Yang, B. Sarsenbekuly, M. Zhang, H. Jiang, W. Kang, S. Aidarova, The advances of organic chromium based polymer gels and their application in improved oil recovery, Adv. Colloid Interface Sci., 282 (2020) 102214, doi: 10.1016/j.cis.2020.102214.
[4] G. Durai, M. Rajasimman, Biological treatment of tannery wastewater – a review, J. Environ. Sci. Technol., 4 (2011) 1–17.
[5] A. Cassano, L.D. Pietra, Drioli, Integrated membrane process for the recovery of chromium salts from tannery effluents, Ind. Eng. Chem. Res., 46 (2007) 6825–6830.
[6] Y. Tang, J. Zhao, Y. Zhang, J. Zhou, B. Shi, Conversion of tannery solid waste to an adsorbent for high-efficiency dye removal from tannery wastewater: a road to circular utilization, Chemosphere, 263 (2021) 127987, doi: 10.1016/j.chemosphere.2020.127987.
[7] S. Sharma, A. Adholeya, Detoxification and accumulation of chromium from tannery effluent and spent chrome effluent by *Paecilomyces lilacinus* fungi, Int. Biodeterior. Biodegrad., 65 (2011) 309–317.
[8] N.K. Mondal, S. Chakraborty, Adsorption of Cr(VI) from aqueous solution on graphene oxide (GO) prepared from graphite: equilibrium, kinetic and thermodynamic studies, Appl. Water Sci., 10 (2020) 61, doi: 10.1007/s13201-020-1142-2.
[9] T.S. Anirudhan, P.G. Radhakrishnan, Chromium(III) removal from water and wastewater using a carboxylate-functionalized cation exchanger prepared from a lignocellulosic residue, J. Colloid Interface Sci., 15 (2007) 268–276.
[10] J. Li, M. Fan, M. Li, X. Lium, Cr(VI) removal from groundwater using double surfactant-modified nanoscale zero-valent iron (nZVI): effects of materials in different status, Sci. Total Environ., 717 (2020) 137112, doi: 10.1016/j.scitotenv.2020.137112.
[11] E. Abu-Dansoa, S. Peraniemi, T. Leiviska, T.Y. Kim, K.M. Tripathi, A. Bhatnagara, Synthesis of clay-cellulose biocomposite for the removal of toxic metal ions from aqueous medium, J. Hazard. Mater., 381 (2020) 120871–120882.
[12] S. Sarode, P. Upadhyay, M.A. Khosa, T. Mak, A. Shakir, S. Song, A. Ullah, Overview of wastewater treatment methods with special focus on biopolymer chitin-chitosan, Int. J. Biol. Macromol., 121 (2019) 1086–1100.
[13] C.P.J. Isaac, A. Sivakumar, Removal of lead and cadmium ions from water using *Annona squamosa* shell: kinetic and equilibrium studies, Desal. Water Treat., 51 (2013) 7700–7709.
[14] T.A. Saleh, Nanocomposite of carbon nanotubes/silica nanoparticles and their use for adsorption of Pb(II): from surface properties to sorption mechanism, Desal. Water Treat., 57 (2016) 10730–10744.
[15] T.A. Saleh, Advanced trends of shale inhibitors for enhanced properties of water-based drilling fluid, Upstream Oil Gas Technol., 8 (2022) 100069, doi: 10.1016/j.upstre.2022.100069.
[16] T.A. Saleh, Experimental and analytical methods for testing inhibitors and fluids in water-based drilling environments, TrAC, Trends Anal. Chem., 149 (2022) 116543, doi: 10.1016/j.trac.2022.116543.
[17] T.A. Saleh, Isotherm, kinetic, and thermodynamic studies on Hg(II) adsorption from aqueous solution by silica- multiwall carbon nanotubes, Environ. Sci. Pollut. Res., 22 (2015) 16721–16731.
[18] M. Belhachemi, F. Addoun, Adsorption of Congo red onto activated carbons having different surface properties: studies of kinetics and adsorption equilibrium, Desal. Water Treat., 37 (2012) 122–129.
[19] T.A. Saleh, A.M. Musa, S.A. Ali, Synthesis of hydrophobic cross-linked polyzwitterionic acid for simultaneous sorption of Eriochrome black T and chromium ions from binary hazardous waters, J. Colloid Interface Sci., 468 (2016) 324–333.
[20] O.A. Bin-Dahman, T.A. Saleh, Synthesis of polyamide grafted on biosupport as polymeric adsorbents for the removal of dye and metal ions, Biomass Convers. Biorefin., (2022), doi: 10.1007/s13399-022-02382-8.
[21] A.A. Basaleh, M.H. Al-Malack, T.A. Saleh, Polyamide-baghouse dust nanocomposite for removal of methylene blue and metals: characterization, kinetic, thermodynamic and regeneration, Chin. J. Chem. Eng., 39 (2021) 112–125.
[22] A.C. Gonçalves Jr., D. Schwantes, M.A. Campagnolo, D.C. Dragunski, C.R.T. Tarley, A.K.D.S. Silva, Removal of toxic

metals using endocarp of açaí berry as biosorbent, Water Sci. Technol., 77 (2018) 1547–1557.
[23] K.R. Jena, Studies on the removal of Pb(II) from wastewater by activated carbon developed from neem wood activated with sulphuric acid, Int. J. Eng. Sci. Res., 2 (2012) 382–394.
[24] H. Panda, N. Tiadi, M. Mohanty, C.R. Mohanty, Studies on adsorption behavior of an industrial waste for removal of chromium from aqueous solution, S. Afr. J. Chem. Eng., 23 (2017) 132–138.
[25] Z.Z. Chowdhury, S.M. Zain, R.A. Khan, M.S. Islam, Preparation and characterizations of activated carbon from kenaf fiber for equilibrium adsorption studies of copper from wastewater, Korean J. Chem. Eng., 29 (2012) 1187–1195.
[26] T.A. Saleh, Simultaneous adsorptive desulfurization of diesel fuel over bimetallic nanoparticles loaded on activated carbon, J. Cleaner Prod., 172 (2018) 2123–2132.
[27] T.A. Saleh, The influence of treatment temperature on the acidity of MWCNT oxidized by HNO_3 or a mixture of HNO_3/H_2SO_4, Appl. Surf. Sci., 257 (2011) 7746–7751.
[28] Z. Xiao, W. Chen, K. Liu, P. Cui, D. Zhan, Porous biomass carbon derived from peanut shells as electrode materials with enhanced electrochemical performance for super capacitors, Int. J. Electrochem. Sci., 13 (2018) 5370–5381.
[29] A. Demirbas, Adsorption of Cr(III) and Cr(VI) ions from aqueous solutions on to modified lignin, Energy Sources, 27 (2005) 1449–1455.
[30] S. Deng, R. Bai, Removal of trivalent and hexavalent chromium with aminated polyacrylonitrile fibers: performance and mechanisms, Water Res., 38 (2004) 2424–2432.
[31] Y. Wu, S. Zhang, X. Guo, H. Huang, Adsorption of chromium(III) on lignin, Bioresour. Technol., 99 (2008) 7709–7715.
[32] V.C.G. Dos Santos, A. de Pádua Andrade Salvado, D.C. Dragunski, D.N. Clausen, C.R.T. Tarley, J. Caetano, Highly improved chromium(III) uptake capacity in modified sugarcane bagasse using different chemical treatments, Quim. Nova, 35 (2012) 1606–1611.
[33] A.Y. Dursun, A comparative study on determination of the equilibrium, kinetic and thermodynamic parameters of biosorption of copper(II) and lead(II) ions onto pretreated *Aspergillus niger*, Biochem. Eng. J., 28 (2006) 187–195.
[34] I. Langmuir, The adsorption of gases on plane surfaces of glass, mica and platinum, J. Am. Chem. Soc., 40 (1918) 1361–1403.
[35] H.M.F.U. Freundlich, Die Adsorption in Losungen, Z. fur. Physikal. Chem., 57 (1906) 385–470.
[36] K.R. Hall, L.C. Eagletonm, A. Acrivos, T. Vermeulen, Pore- and solid-diffusion kinetics in fixed-bed adsorption under constant-pattern conditions, Ind. Eng. Chem. Fundam., 5 (1966) 212–223.
[37] M. Hua, S. Zhang, B. Pan, W. Zhang, L. Lv, Q. Zhang, Heavy metal removal from water/wastewater by nanosized metal oxides: a review, J. Hazard. Mater., 15 (2012) 211–212: 317–331.
[38] D. Božić, M. Gorgievski, V. Stanković, N. Štrbac, S. Šerbula, N. Petrović, Adsorption of heavy metal ions by beech sawdust – kinetics, mechanism and equilibrium of the process, Ecol. Eng., 58 (2013) 202–206.
[39] Y.S. Ho, J.C.Y. Ng, G. McKay, Kinetics of pollutant sorption by biosorbents: review, Sep. Purif. Methods, 29 (2000) 189–232.
[40] J. Kong, Q. Yue, S. Sun, B. Gao, Y. Kan, Q. Li, Y. Wang, Adsorption of Pb(II) from aqueous solution using keratin waste–hide waste: equilibrium, kinetic and thermodynamic modeling studies, Chem. Eng. J., 241 (2014) 393–400.
[41] S. Parlayicim, E. Pehlivan, Comparative study of Cr(VI) removal by bio-waste adsorbents: equilibrium, kinetics, and thermodynamic, J. Anal. Sci. Technol., 10 (2019) 15, doi: 10.1186/s40543-019-0175-3.
[42] Z. Droussi, V. D'Orazio, M.R. Provenzano, M. Hafidi, A. Ouatmane, Study of the biodegradation and transformation of olive-mill residues during composting using FTIR spectroscopy and differential scanning calorimetry, J. Hazard. Mater., 164 (2009) 1281–1285.
[43] R. Shan, Y. Shi, J. Gu, Y. Wang, H. Yuan, Single and competitive adsorption affinity of heavy metals toward peanut shell-derived biochar and its mechanisms in aqueous systems, Chin. J. Chem. Eng., 28 (2020) 1375–1383.
[44] F. Albert Cotton, J. Takats, Structure of triphenylphosphine-(pentahaptocyclopentadienyl) copper(I), J. Am. Chem. Soc., 92 (1970) 2353–2358.